

Decontamination of Aqueous Glyphosate, (Aminomethyl) phosphonic Acid, and Glufosinate Solutions by Electro-Fenton-like Process with Mn^{2+} as the Catalyst

BEYTUL BALCI, MEHMET A. OTURAN, NIHAL OTURAN, AND IGNASI SIRÉS*

Université Paris-Est, Laboratoire Géomatériaux et Géologie de l'Ingénieur, 5 Bd Descartes,
77454 Marne-la-Vallée Cedex 2, France

The ability of the modified electro-Fenton-like (EF-like) process to degrade aqueous solutions of glyphosate, which is the most widely used herbicide in the world, has been assessed with Mn^{2+} and other metal ions as catalysts to overcome the problems posed by some stable metal ion complexes of phosphonate herbicides. Bulk electrolyses with a carbon-felt cathode and Pt anode were performed in an undivided cell under galvanostatic conditions to study the effect of the applied current as well as Mn^{2+} and glyphosate concentrations. The herbicide was completely destroyed in all cases following a pseudofirst-order kinetics, and the second-order rate constant for its reaction with $\cdot OH$ was determined. The decay trends obtained by high-performance liquid chromatography–fluorometric detection (HPLC-FL) and ion chromatography analysis were similar. AMPA [(aminomethyl)phosphonic acid] was the major reaction intermediate and showed slower pseudofirst-order destruction kinetics. The high mineralization degree obtained for glyphosate solutions confirmed the great performance of the EF-like process with Mn^{2+} , which promotes the C–N cleavage by $\cdot OH$ attack as the first oxidation step and the C–P cleavage in a further step. High-level decontamination achieved for AMPA and glufosinate solutions corroborated the benefits of this oxidation process.

KEYWORDS: Glyphosate; phosphonate herbicides; electro-Fenton process; Fenton-like process; manganese; water treatment

INTRODUCTION

Pesticide pollution of the aquatic environment is a major concern for our society because of the potential adverse effects of these compounds to ecosystems and humans (1). Organophosphorous (OP) pesticides are usually preferred rather than organochlorine ones because they show a lower persistence and bioaccumulation and a higher biodegradability (2). Phosphonates and amino acid group-containing pesticides such as glufosinate and glyphosate, which are broad spectrum, nonselective, and postemergence herbicides for the control of long grasses and broad-leaved weeds, constitute an important category among those OP (3), and their continued use raises the potential for residue accumulation in both soil through adsorption (4, 5) and water due to their high solubility and leaching (5).

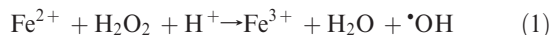
Glufosinate is a site preparation herbicide readily biotransformed in soil, with 3-(methylphosphinyl)propionic acid (MPPA) as the main metabolite (3). Glyphosate, first marketed by Monsanto as Roundup (6), has become the world's leading agrochemical (7), especially in recent years with the widespread of genetically modified glyphosate-tolerant crops (8), and its physical, chemical, environmental, and toxicological properties have been well-documented (8–11). It is rapidly degraded by soil microorganisms, yielding glyoxylate and (aminomethyl)

phosphonic acid (AMPA) as primary intermediates (3, 4). AMPA is more toxic than the parent molecule and more persistent in water and soil (4). In conclusion, wastewater treatment technologies other than bioremediation are required for the quick and high removal of these mobile persistent organic pollutants (POPs), but literature is somewhat scarce. As far as we know, no abiotic treatments have been reported for the degradation of glufosinate, whereas photo-Fenton process (12), photodegradation in the presence of ferrioxalate (13), photocatalysis with TiO_2 (14), oxidation by manganese oxide (6, 15), and electrooxidation with DSA anodes (16) have been used for the removal of AMPA and/or glyphosate from aqueous solutions.

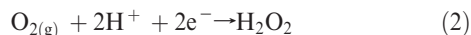
In recent years, the electrochemical technology has received significant attention to overcome the inefficiency of conventional wastewater treatment, since it possesses certain particular properties that make it appealing: secure and easy handling, amenability of automation, versatility, and environment compatibility (17), as well as increasing cost-effectiveness due to the constant improvement of the electrode materials and hydrodynamic conditions. Several electrochemical advanced oxidation processes (EAOPs), which are based on the action of oxidant hydroxyl radical [$E^\circ(\cdot OH/H_2O) = 2.8 \text{ V/NHE}$], have shown the possibility to reach a high degree of conversion of pollutants, even up to their complete mineralization. The great performance of both direct anodic oxidation (AO) and indirect EAOPs based on Fenton's reaction 1 between iron catalyst and hydrogen peroxide

*To whom correspondence should be addressed. Tel: +33 149 32 90 60. Fax: +33 149 32 91 37. E-mail: isires@catalonia.net.

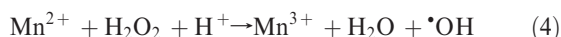
(i.e., Fenton's reagent) for the degradation of POPs by $\cdot\text{OH}$ allows justification of the notorious expansion of this area (16, 18–31):



Indirect EAOPs are very interesting because the production of high amounts of $\cdot\text{OH}$ in the bulk solution allows minimization of the limitations associated with mass transfer of organics. Electro-Fenton (EF) process with in situ electrogeneration of H_2O_2 from reaction 2 is the most ecofriendly technique among them, since it prevents handling, storage, and transportation of such a chemical, and catalysis with iron ions has led to very promising results regarding water remediation (18, 20–22, 24–26, 28–31). Recently, we have demonstrated that the use of three-dimensional cathodes greatly accelerates and enhances the degradation process because the continuous regeneration of Fe^{2+} from reaction 3 maintains the catalytic cycle (25, 29–31):



A serious inconvenience arises when treating iron-chelating organic compounds, because an iron catalyst needed to carry out Fenton's reaction 1 is no longer available and the process becomes ineffective. This is the case of phosphonates, which are able to form stable complexes with most transition metal cations through their amine, carboxylate, and phosphonate groups (32). Most of them are insoluble (33, 34), but phosphonate complexes with manganese are relatively weak and can be degraded (6, 15). Consequently, we propose the use of a Mn^{2+} -mediated EF process that we call EF-like process because, similarly to Fenton-like process (35), it is based on the action of a catalyst different from Fe^{2+} on H_2O_2 , as shown in reaction 4 and regeneration reaction 5:



In this work, bulk electrolyses of 200 mL of acidic aqueous polluted solutions have been carried out with a three-dimensional carbon-felt cathode and Pt anode in an undivided electrolytic cell to study the performance of Mn^{2+} -mediated EF-like process for the degradation of glyphosate. There exist serious difficulties for the analysis of phosphonates due to their high polarity and water solubility, insolubility in organic solvents, favored complexing ability, and absence of a chromophore or fluorophore group in their structure (3). Thus, high-performance liquid chromatography (HPLC) analysis with precolumn derivatization and fluorimetric detection (FL) has been used, and it has been compared to ion chromatography (IC) analysis, aiming to use a quicker, simpler, and sensitive method to monitor glyphosate. The effect of applied current and initial concentration of glyphosate and Mn^{2+} is discussed, and the second-order rate constant between glyphosate and $\cdot\text{OH}$ is determined. AMPA and glufosinate solutions have been treated as well to confirm the oxidation ability of the EF-like process. Finally, a reaction pathway for the mineralization of glyphosate is proposed based on the intermediates identified.

MATERIALS AND METHODS

Chemicals. Glyphosate [*N*-(phosphonomethyl)glycine] and glufosinate-ammonium [2-amino-4-(hydroxymethylphosphinyl)butanoic acid ammonium salt] were Pestanal standards from Fluka, whereas AMPA was analytical grade from Aldrich (purity $\geq 99\%$), and they were used

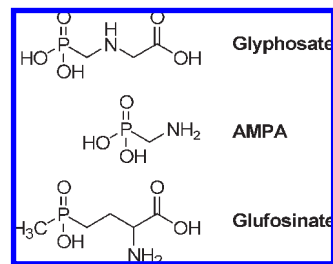


Figure 1. Chemical structures for the three compounds studied.

without further purification. Their structures are shown in Figure 1. Formic, glycolic, glyoxylic, oxalic, and sulfuric acids and anhydrous sodium sulfate were either reagent or analytical grade from Fluka and Acros Organics. Silver sulfate, cobalt(II) sulfate heptahydrate, ferrous sulfate heptahydrate, ferric sulfate pentahydrate, and manganese(II) sulfate monohydrate used as catalyst sources were either reagent or analytical grade ($\geq 99\%$) from Sigma-Aldrich and Acros Organics. Borax anhydrous ($\text{Na}_2\text{B}_4\text{O}_7$, $\geq 98\%$) and FMOC-Cl (9-fluorenylmethoxycarbonyl chloride, $\geq 99\%$) used for derivatization and heptafluorobutyric acid ($\geq 99.5\%$) used for IC were from Fluka. Other reagents used for the chromatographic and total organic carbon (TOC) analyses were high purity from Sigma-Aldrich and Acros Organics. All solutions were prepared in ultrapure water obtained from a Millipore Milli-Q system with resistivity $> 18 \text{ M}\Omega \text{ cm}$ at room temperature.

EF-Like Treatments. Bulk electrolyses were conducted in an open, cylindrical, and undivided glass cell of 6 cm diameter and 250 mL capacity described in previous studies, with a 4.5 cm^2 Pt cylindrical mesh as the anode and a 60 cm^2 ($15 \text{ cm} \times 4 \text{ cm}$) carbon felt from Carbone-Lorraine exposed on both sides as the cathode (30). The anode was centered in the electrolytic cell surrounded by the cathode, which covered the inner wall of the cell and produced H_2O_2 from reduction of O_2 dissolved in the solution according to reaction 2. Continuous saturation of this gas was ensured by bubbling compressed air having passed through a frit at about 1 L min^{-1} , starting 10 min before electrolysis to reach a stationary O_2 concentration.

Solutions of 200 mL containing glyphosate, AMPA, or glufosinate with $0.05 \text{ M Na}_2\text{SO}_4$ as the background electrolyte and a selected amount of Mn^{2+} ions as catalysts at pH 3.0 adjusted with H_2SO_4 were degraded at room temperature ($23 \pm 2 \text{ }^\circ\text{C}$) and at constant current supplied by an EG&G Princeton Applied Research 273A potentiostat/galvanostat. The value of pH 3.0, quite stable along the treatments, was measured with an Eutech Instruments CyberScan pH 1500 pH meter and was selected as the optimum one to carry out Fenton's and Fenton-like reactions, according to several studies on the optimization of EF process (25, 29, 30). All solutions were vigorously stirred with a magnetic bar to enhance mass transfer of all reagents. For comparison, other EF and EF-like processes with Fe^{2+} , Fe^{3+} , Cu^{2+} , Ag^+ , or Co^{2+} as catalysts were tested as well.

Analytical Techniques and Procedures. First, the evolution of glyphosate and AMPA was followed by reversed-phase HPLC, which requires a protocol of pre- or postcolumn derivatization. In this work, the use of FMOC-Cl as the precolumn derivatization agent yielded the corresponding fluorescent derivatives. Briefly, the samples (3 mL) withdrawn throughout electrolysis were collected in polypropylene bottles and derivatized by adding a buffer solution of 0.05 mM borax and 1 g L^{-1} FMOC-Cl solution. The reaction was carried out with agitation at the ambient temperature for 1 h. The derivatization reagent in excess was eliminated by washing the samples with diethyl ether, and the aqueous phase was recovered for the direct injection into the HPLC-FL system (36). The monitoring was conducted with a Merck Lachrom liquid chromatograph equipped with a L-7100 pump, fitted with a Equisorb $5 \mu\text{m}$, $25 \text{ cm} \times 4.6 \text{ mm}$ (i.d.), column at $40 \text{ }^\circ\text{C}$, and coupled with a fluorescence detector selected at $\lambda_{\text{exc}} = 265 \text{ nm}$ and $\lambda_{\text{em}} = 315 \text{ nm}$. Analysis was carried out isocratically by using a 45:55 (v/v) acetonitrile/phosphate buffer solution (pH 5.75) mixture, at a flow rate of 1 mL min^{-1} . Samples of $20 \mu\text{L}$ were injected into the liquid chromatograph, and measurements were controlled through EZChrom Elite 3.1 software. Standards of glyphosate and AMPA, which appeared at retention times of 17.2 and 4.2 min, respectively, were analyzed following the same methodology to obtain their external calibration curves. A standard addition method was used to confirm each peak and carry out a more accurate quantification.

Although HPLC-FL analysis allows the selective, highly sensitive, and highly accurate determination of glyphosate and AMPA, this method has not received wide acceptance because of complex instrumentation and unconventional reagents. Thus, on the basis of the charged nature of glyphosate, its decay was alternatively determined by IC using a Dionex ICS 1000 system fitted with an IonPac ICE-AS1, 25 cm \times 9 mm, acidic column, linked to a column guard, and coupled with a DS6 conductivity detector containing a cell heated at 35 $^{\circ}$ C under control through Chromeleon SE software. The sensitivity of this detector was improved from electrochemical suppression. Measurements were conducted by injecting 25 μ L of the samples, with 1 mM heptafluorobutyric acid solution circulating at 0.8 mL min^{-1} as the mobile phase. Note that the literature is very poor concerning the analysis of the glyphosate without derivatization (3, 37).

Final short-chain carboxylic acids were identified and quantified by ion-exclusion HPLC using the same Merck Lachrom liquid chromatograph equipped with an L-2130 pump, fitted with a Supelco Supelcogel H, 9 μ m, 25 cm \times 4.6 mm (i.d.), column at 40 $^{\circ}$ C, and coupled with a L-2400 UV detector selected at $\lambda = 210$ nm. The mobile phase was 4 mM H_2SO_4 at 0.2 mL min^{-1} , and oxalic, glyoxylic, glycolic, and formic acids appeared at 7.5, 11.4, 15.1, and 16.0 min, respectively.

The mineralization of glyphosate, AMPA, and glufosinate solutions was monitored by their TOC abatement, determined on a Shimadzu VCSH TOC analyzer, using the standard nonpurgeable organic carbon method. Samples were microfiltered onto a hydrophilic membrane (Millex-GV Millipore, 0.22 μ m) prior to analysis.

RESULTS AND DISCUSSION

Removal of Glyphosate by EF-Like Process with Mn^{2+} . The degradation of acidic aqueous solutions of 0.1 mM glyphosate was first studied with 0.1 mM of different metal ions as catalysts at a constant current of 100 mA, employing HPLC-FL as an analytical method. Ferrous and ferric ions were used to test the viability of the classical EF process that is based on the electrochemically assisted Fenton's reaction 1. Foam was already formed at short electrolysis time, and insoluble particles progressively yielded a precipitate that prevented the degradation of glyphosate, thus confirming that strong complexes of the herbicide with metal ions are sometimes produced. Next, EF-like treatments were carried out with Ag^+ and Co^{2+} . As depicted in **Figure 2a**, they led to a very slow decay and a poor degree of glyphosate destruction at 180 min, equal to 33 and 31% for Ag^+ and Co^{2+} , respectively. The effect of copper ions was even worse (not shown), as reported elsewhere (6).

The disappearance of glyphosate is accompanied by the formation of its main degradation product, that is, AMPA, without any other product observed. As shown in the inset of **Figure 2a**, AMPA is formed from the beginning of the electrolysis, and it is very slowly degraded along the treatment, which suggests a low reactivity with $\cdot\text{OH}$. Its destruction is almost complete at 420 min.

On the basis of the positive effect of Mn^{2+} ions reported in some studies referred to in the Introduction, we used this species with the aim of achieving better results. The effect of Mn^{2+} concentration was studied for the degradation of 0.1 mM glyphosate at 100 mA. In contrast to the aforementioned results, overall destruction of the herbicide was achieved in all cases, although different trends were obtained. At 40 min, for example, the decay was 89, 92, 80, and 74% for 0.05, 0.1, 0.5, and 1 mM Mn^{2+} , respectively, as can be seen in **Figure 2b**. Thus, the decay with 0.1 mM Mn^{2+} as the catalyst in EF-like process was the quickest one, with a total disappearance of glyphosate at 180 min, as shown in **Figure 2a**. The formation of large amounts of the very oxidizing agent $\cdot\text{OH}$ in the bulk solution from reaction 4 accounts for the effective oxidation of the pollutant in such EF-like treatment. Moreover, the three-dimensional cathode contributes to continuously regenerate the Mn^{2+} required, as suggested in

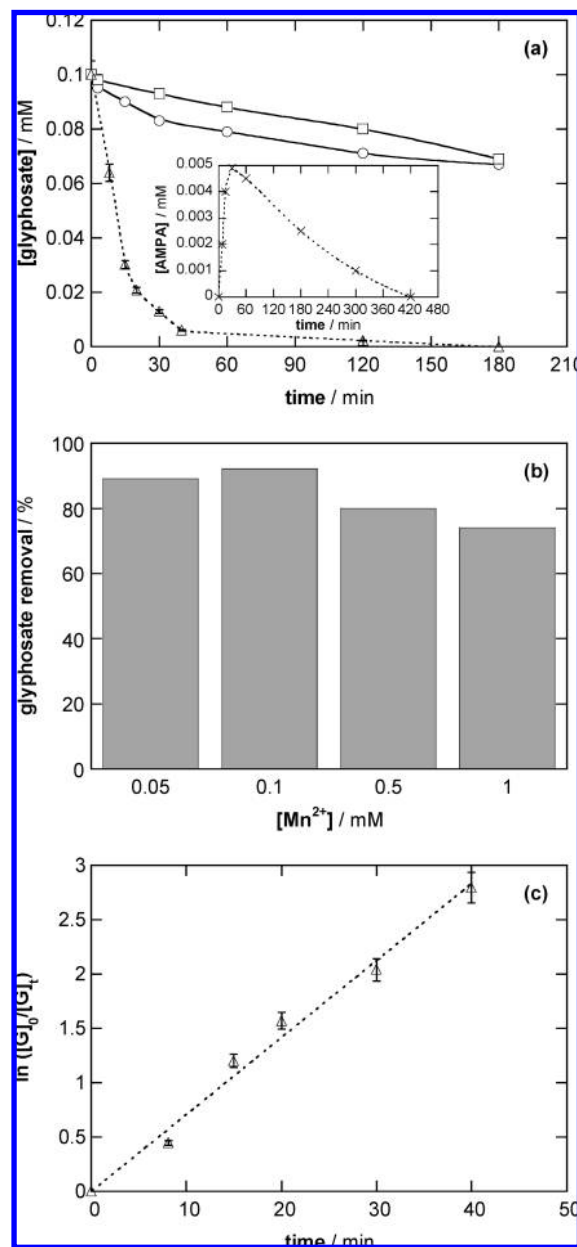


Figure 2. (a) Decay of glyphosate concentration with time, determined by HPLC-FL, for the treatment of solutions of 200 mL containing 0.1 mM herbicide in 0.05 M Na_2SO_4 at 100 mA, pH 3.0, and room temperature by EF-like process with 0.1 mM catalyst: Ag^+ (\circ), Co^{2+} (\square), and Mn^{2+} (\triangle). Symbols are the experimental data; lines are smooth trend fittings. The error bars indicate the 3% range for concentration data obtained by IC analysis as compared to HPLC-FL. The inset panel shows the time course of the concentration of AMPA formed during the previous treatment with Mn^{2+} . (b) Percentage of glyphosate removal attained after 40 min of an EF-like process under the conditions detailed in plot a, with the Mn^{2+} concentration between 0.05 and 1 mM. (c) Kinetic analysis for the decays with Mn^{2+} shown in plot a, assuming a pseudofirst-order behavior.

reaction 5. The fact that an increasing catalyst concentration up to 0.1 mM leads to a quicker degradation, whereas further increase is detrimental, can be explained by the progressive enhancement of quick parallel nonoxidizing reactions between $\cdot\text{OH}$ and Mn^{n+} , similarly to parasitic reactions reported for traditional EF process with iron ions (25, 29, 30). The coexistence of such reactions leads to the progressive fall of the amount of $\cdot\text{OH}$ really available to carry out the oxidation of organics at high Mn^{2+} concentrations because some Mn^{2+} will react with

$\cdot\text{OH}$ instead of participating in reaction 4. In addition, an increasing Mn^{2+} concentration causes a greater complexation of the herbicide, thus reducing the relative amount of free glyphosate that can react quickly with $\cdot\text{OH}$. In conclusion, the process is optimum with a catalytic amount of Mn^{2+} able to catalyze the oxidation process as well as minimize undesirable side reactions. In contrast, a nonelectrochemical Fenton-like process with Mn^{2+} and added H_2O_2 has been proven to yield poor decontamination of solutions containing several pollutants (38). On the other hand, note that the time required for total destruction is large if compared to EF treatment of other pollutants with iron as the catalyst (22, 25, 26, 29–31). This can be due to (i) the complexation of some of the Mn^{2+} ions, which makes them unavailable to carry out reaction 4, and (ii) the slower reaction rate of reaction 4 as compared to Fenton's reaction 1. This latter argument has been demonstrated by some authors, who stated that $\cdot\text{OH}$ production in Fenton-like systems with soluble manganese proceeds more slowly than using iron as the catalyst (35).

Because HPLC-FL analysis with precolumn derivatization involves quite a complicated and time-consuming methodology, a simpler and quicker technique such as IC was employed for comparison, based on the fact that glyphosate behaves like a moderately strong acid with $\text{p}K_{\text{a}1}$, $\text{p}K_{\text{a}2}$, $\text{p}K_{\text{a}3}$, and $\text{p}K_{\text{a}4}$ of 0.78, 2.29, 5.96, and 10.98, respectively, so it is ionized at pH 3. The results obtained for the degradation of glyphosate with Mn^{2+} were very similar to those already commented, yielding concentration values that differed only up to 3% as maximum from the previous ones. This fact is represented in **Figure 2a** by displaying the corresponding 3% error bars for each experimental point in the decay with Mn^{2+} . Therefore, the results presented hereafter for the time course of glyphosate are based on IC analysis.

On the other hand, the kinetic analysis for the EF-like treatment of glyphosate with 0.1 mM Mn^{2+} yielded a pseudo-first-order kinetics for its degradation with $\cdot\text{OH}$, as presented in **Figure 2c**, which means that a constant concentration of oxidizing agent is produced from reaction 4. The calculated apparent rate constant for glyphosate ($k_{\text{app}(\text{G})}$) was found to be 0.071 min^{-1} , showing excellent linear correlation ($R^2 = 0.994$).

The effect of the initial concentration of glyphosate was studied by EF-like process with 0.1 mM Mn^{2+} at 200 mA, using 0.1, 0.2, or 0.4 mM glyphosate. The treatment is very effective because total destruction is always reached, but as depicted in **Figure 3**, increasing the time to 60, 90, and 480 min is required as the initial concentration is higher. Accordingly, the process is quite fast for 0.1 and 0.2 mM but becomes much slower for 0.4 mM. The exponential decays have been analyzed and fitted in the inset of **Figure 3** to a pseudo-first-order decay kinetics that yields decreasing $k_{\text{app}(\text{G})}$ values of 0.086 ($R^2 = 0.997$), 0.039 ($R^2 = 0.999$), and 0.010 ($R^2 = 0.985$) min^{-1} at 0.1, 0.2, and 0.4 mM, respectively. The slower degradation at higher initial concentration of pollutant can be explained by (i) the formation of a greater amount of oxidation byproducts, which compete with glyphosate to react with the stationary concentration of $\cdot\text{OH}$, and (ii) the lower concentration of free Mn^{2+} in the bulk solution because of the progressively greater complexation with rising amounts of the herbicide, leading to a lower generation of $\cdot\text{OH}$ along with a lower relative proportion of free glyphosate. Note that a higher concentration of glyphosate is detrimental for the destruction kinetics of the herbicide, but at the same time, it accelerates the decontamination of the solution because of the concomitant oxidation of both the initial pollutant and its intermediates, so the efficiency of the decontamination treatment increases. This was also found during the treatment of increasing concentrations of pesticides and dyes (26, 29).

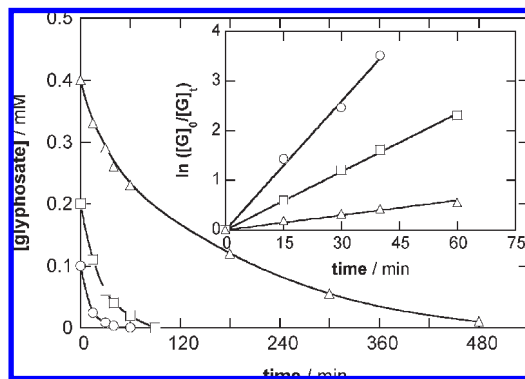


Figure 3. Effect of initial glyphosate concentration on destruction kinetics with electrolysis time for EF-like treatment of herbicide solutions with 0.05 M Na_2SO_4 and 0.1 mM Mn^{2+} at 200 mA, pH 3.0, and room temperature. $[\text{Glyphosate}]_0$: 0.1 (○), 0.2 (□), and 0.4 mM (△). The corresponding kinetic analyses assuming a pseudo-first-order decay kinetics for glyphosate are given in the inset panel.

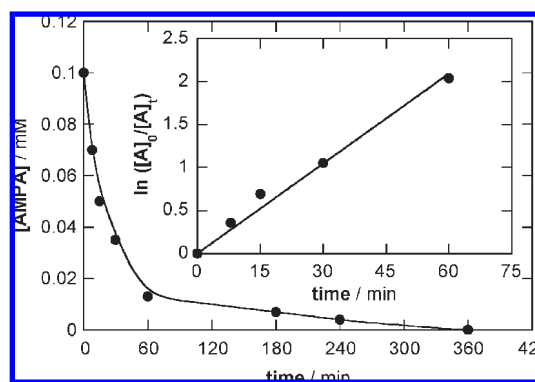


Figure 4. Decay of AMPA vs time for the EF-like treatment of solutions of 200 mL containing 0.1 mM AMPA with 0.05 M Na_2SO_4 and 0.1 mM Mn^{2+} at 250 mA, pH 3.0, and room temperature. The inset shows the corresponding kinetics analysis.

From the kinetic analysis presented in **Figure 2c** and **3**, it is also possible to assess the effect of the applied current during the treatment of 0.1 mM glyphosate. The $k_{\text{app}(\text{G})}$ values at 100 and 200 mA are 0.071 and 0.086 min^{-1} , respectively. As expected from the quicker electrogeneration of H_2O_2 and Mn^{2+} as the current rises, which yields increasing amounts of $\cdot\text{OH}$ from reaction 4 at a given time, a quicker destruction of the herbicide is observed at a higher current, with a shorter electrolysis time needed for total destruction. However, the rate constant does not rise proportionally to the applied current due to the parasitic reactions noted above that increase the relative proportion of wasted $\cdot\text{OH}$.

Given the importance of AMPA as a primary intermediate during the EF-like treatment of glyphosate, its degradation was studied as well by electrolyzing a solution containing 0.1 mM AMPA and 0.1 mM Mn^{2+} at 250 mA. **Figure 4** shows a slow exponential decay of AMPA until it disappears at 360 min. Such slowness agrees with the time course of AMPA discussed in **Figure 2a** and other studies on the removal of AMPA (6). From the inset, it is evident that its oxidation reaction follows a pseudo-first-order equation, with $k_{\text{app}(\text{AMPA})}$ of 0.035 min^{-1} ($R^2 = 0.992$), which is about half the value found for glyphosate at 100 mA.

Determination of the Absolute Rate Constant of Glyphosate. The second-order or absolute rate constant for the reaction between glyphosate and $\cdot\text{OH}$ was determined by means of the competition kinetics method (39), taking benzoic acid (BA) as the standard competition substrate whose absolute rate constant with $\cdot\text{OH}$ is

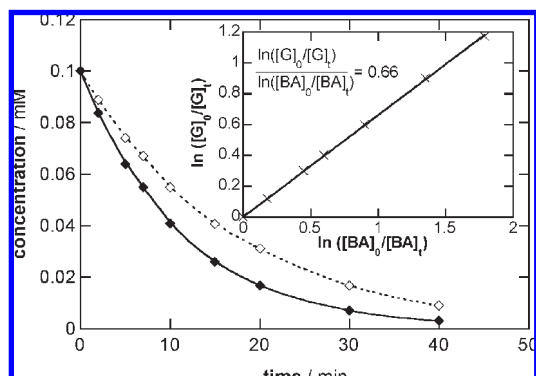


Figure 5. Decay of glyphosate (\diamond) and benzoic acid (\blacklozenge) concentration during the determination of the absolute rate constant between glyphosate and $\cdot\text{OH}$ by the competition kinetics method. EF-like experiments were carried out with solutions of 200 mL containing 0.1 mM glyphosate and 0.1 mM benzoic acid with 0.05 M Na_2SO_4 and 0.1 mM Mn^{2+} at 100 mA, pH 3.0, and room temperature. The inset shows the corresponding kinetic analysis.

well-established ($k_{\text{BA}} = 4.30 \times 10^9 \text{ M}^{-1} \text{ s}^{-1}$). Briefly, solutions containing 0.1 mM BA and 0.1 mM glyphosate with 0.1 mM Mn^{2+} were electrolyzed at 100 mA, and the evolution of the corresponding peaks was followed for short reaction times by reversed-phase HPLC. BA and glyphosate concentrations decreased exponentially in both cases, as observed in **Figure 5**, so it was possible to simultaneously determine the apparent rate constants for the pseudofirst-order reactions of BA ($k_{\text{app(BA)}} = 0.089 \text{ min}^{-1}$) and glyphosate ($k_{\text{app(G)}} = 0.059 \text{ min}^{-1}$) with $\cdot\text{OH}$. It is worth noting the lower rate constant value for glyphosate in the presence of BA as compared to that obtained from **Figure 2c**, which confirms the competitive role of byproducts suggested to explain the trends at a high concentration of glyphosate in **Figure 3**. The determination of both apparent rate constants is not really necessary for the calculation of glyphosate oxidation reaction rate constant, which can be obtained from the representation shown in the inset of **Figure 5**, that yields a value of 0.66 ($R^2 = 0.998$) for the slope, along with the following relationship:

$$k_{\text{G}} = k_{\text{BA}} \times \frac{k_{\text{app(G)}}}{k_{\text{app(BA)}}} = k_{\text{BA}} \times \frac{\ln\left(\frac{[\text{G}]_0}{[\text{G}]_t}\right)}{\ln\left(\frac{[\text{BA}]_0}{[\text{BA}]_t}\right)} \quad (6)$$

The absolute constant found for glyphosate is $k_{\text{G}} = 2.8 \times 10^9 \text{ M}^{-1} \text{ s}^{-1}$. Haag and Yao also used the competition kinetics method, with glycolic acid as the reference compound, and obtained $k_{\text{G}} = 1.8 \times 10^8 \text{ M}^{-1} \text{ s}^{-1}$ for the photo-Fenton degradation of the herbicide with Fe^{3+} ions at pH about 3 (40). They cautioned that the rate constant may have been affected by complexation with iron, which is evident from our above results, so it can justify the disagreement regarding the calculated values. In addition, the steady-state $\cdot\text{OH}$ concentration generated from reaction 4 can be calculated according to expression 7, which yields an average value of $4 \times 10^{-13} \text{ M}$ at 100 mA. This value is somewhat lower than 1.8×10^{-12} to 2.3×10^{-12} determined by EF process with iron ions (29, 31), thus confirming that the catalytic effect of Mn^{2+} on H_2O_2 is lower than that with iron.

$$k_{\text{app(G)}} = k_{\text{G}} \times [\cdot\text{OH}] \quad (7)$$

Mineralization of Glyphosate, AMPA, and Glufosinate and Proposal of a Reaction Pathway. The ability of the EF-like process to allow the removal of glyphosate, AMPA, and glufosinate, along with their respective oxidation byproducts, was assessed

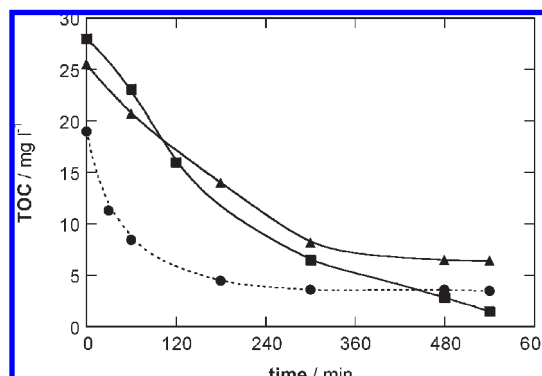


Figure 6. TOC removal vs. electrolysis time for the study of the mineralization of aqueous solutions of 0.5 mM glyphosate (\bullet), 2.0 mM AMPA (\blacksquare), and 0.5 mM glufosinate (\blacktriangle) by EF-like process with 0.05 M Na_2SO_4 and 0.5 mM Mn^{2+} at 500 mA, pH 3.0, and room temperature.

from the mineralization degree achieved for each individual solution based on the TOC removal. The starting acidic aqueous solutions contained 0.5 mM glyphosate, 2.0 mM AMPA, or 0.5 mM glufosinate to start at about 20–25 mg L^{-1} TOC. The electrolyses were carried out for 540 min at high applied current of 500 mA to shorten the total electrolysis time, in the presence of 0.5 mM Mn^{2+} ions as the catalyst to maintain an acceptable catalyst/pollutant ratio. In **Figure 6**, it can be seen that TOC undergoes a progressive decay with time at least for 180 min in all cases. Glyphosate shows the quickest TOC abatement during the first stages, but after reaching 82% TOC removal at about 300 min, it remains almost unchanged, with a residual TOC of about 3.5 mg L^{-1} at 540 min. As for AMPA, a much slower but continuous degradation is observed up to its quasi-total mineralization (>95%). The low mineralization rate agrees with the slow destruction kinetics described in **Figure 4**. In the case of glufosinate, the mineralization rate is lower than that of glyphosate, and also a lower TOC abatement of about 75%, corresponding to a residual TOC of 6.5 mg L^{-1} , is achieved from 360 min. Some factors can account for the lower mineralization rate over time as well as the only partial mineralization of glyphosate and glufosinate: (i) The formation of some byproducts that are more refractory to oxidation, as for example carboxylic acids, which are known to have a relatively low absolute rate constant with $\cdot\text{OH}$ (31); (ii) the existence of some complexes of Mn^{3+} that, similarly to complexes of Fe^{3+} with certain carboxylic acids (22, 25, 26, 31), may not be oxidizable by $\cdot\text{OH}$ in the bulk solution; and (iii) the lower production of $\cdot\text{OH}$ from reaction 4 due to the decrease of free Mn^{2+} , which is mainly caused by the complexation of Mn^{2+} . Some authors have highlighted the importance of the additional role of the Mn^{2+} AO reaction to MnO_2 (31) and Mn^{3+} disproportionation into Mn^{2+} and MnO_2 that is less reactive than soluble ions (38) for systems with manganese, but such collateral reactions can be discarded in our process because the efficient Mn^{n+} cathodic reduction prevents MnO_2 deposition or precipitation.

For comparison, low mineralization of glyphosate was reported elsewhere by photo-Fenton process, with 35% TOC removal in 120 min, suggesting the possible accumulation of persistent OP byproducts (12). On the other hand, only 24% TOC removal was observed for the electrooxidation of glyphosate with RuO_2 - and IrO_2 -based anodes in the absence of chloride ions, whereas almost total mineralization was achieved in chloride medium (16). It can then be concluded that the EF-like treatment with Mn^{2+} yields a high degree of mineralization of all three compounds, which ensures the destruction of the very toxic

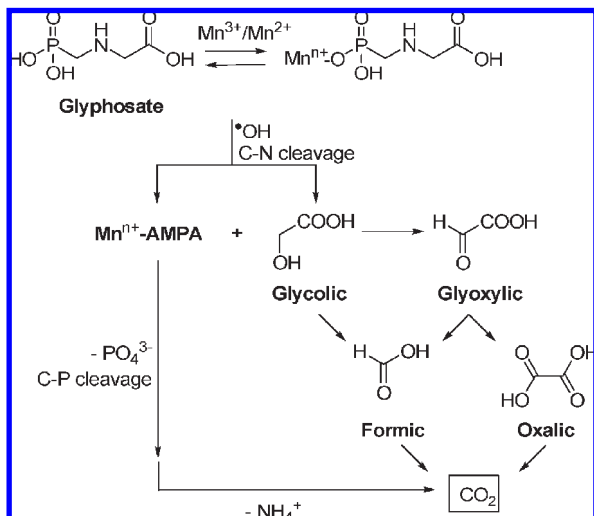


Figure 7. Proposed reaction sequence for the overall mineralization of glyphosate in acidic aqueous medium by EF-like process with Mn^{2+} .

initial pollutant. Coupling with bioremediation methods could be suggested if total TOC removal was required.

Focusing on the treatment of glyphosate, it has been demonstrated that only partial TOC abatement is reached, whereas its primary byproduct AMPA is completely mineralized, which means that other intermediates limit the mineralization process of the herbicide. As deduced from the structures shown in **Figure 1**, short-chain carboxylic acids can be formed during the EF-like treatment. To identify the major carboxylic acids formed during the electrolysis, some EF-like treatments were performed with solutions containing 0.5 mM glyphosate and 0.5 mM Mn^{2+} ions by applying a constant current of 100 mA. This lower value was selected to favor the larger accumulation of intermediates and help their monitoring. Ion-exclusion chromatograms displayed a well-defined peak corresponding to glycolic acid as the first and major carboxylic byproduct. In addition, glyoxylic and oxalic acid were identified in a very small concentration, whereas the formic acid concentration was slightly higher. Following the above explanation, complexes of Mn^{3+} with these intermediates could be hypothesized to be responsible for the limited mineralization of the herbicides under study. As a result of these analyses, a reaction pathway for the complete mineralization of glyphosate is proposed in **Figure 7**, with $\cdot OH$ as the main oxidant. C–N cleavage is promoted by $\cdot OH$ attack onto complexed or uncomplexed glyphosate as the first oxidation step to yield AMPA and glycolic acid, whereas C–P cleavage is given in a further step along with the concomitant oxidation of the released byproducts. Thus, the overall mineralization of AMPA is accompanied by the release of phosphate (PO_4^{3-}) and ammonium (NH_4^+) ions, whereas uncomplexed formic and oxalic acids formed from the oxidation of glycolic acid can also be destroyed by $\cdot OH$. The transformation of glycolic acid into CO_2 through glyoxylic acid agrees with recent results published by us where the significant accumulation of formic acid was reported (31). Phosphate ions were not monitored in this study, but their formation can be inferred from degradation studies of glyphosate based on the action of $\cdot OH$ (12, 16). The release of ammonium as a major nitrogenated product from AMPA degradation is based on findings reported in some papers regarding the fate of nitrogen atoms contained in primary amines during EF treatments (30).

The pathway presented differs from others that propose the primary C–P cleavage during the treatment with manganese oxide (6). Some authors reported the formation of AMPA

and sarcosine (*N*-methylglycine, $CH_3-NH-CH_2-COOH$) as primary intermediates instead (6, 13, 16).

The current study contributes to enlarge the scarce literature on the removal of glyphosate, AMPA, and glufosinate. The electrochemical process called EF-like with Mn^{2+} as the catalyst allows overcoming the difficulties posed by the formation of stable complexes whenever other metal ions are used instead. The process leads to the complete destruction of glyphosate and its main byproduct, as well as a high degree of mineralization of glyphosate, AMPA, and glufosinate. In all cases, the degradation kinetics is slow as compared to EF treatment of other POPs with Fe^{2+} , but the EF-like process constitutes an interesting environmentally friendly alternative in cases like the one discussed, when some limitations prevent the use of the classical EF process.

ACKNOWLEDGMENT

I.S. acknowledges support from the Laboratoire Géomatériaux et Géologie de l'Ingénieur to obtain the ATER position in the Université Paris-Est Marne-la-Vallée.

LITERATURE CITED

- (1) Rice, P. J.; Rice, P. J.; Arthur, E. L.; Barefoot, A. C. Advances in pesticide environmental fate and exposure assessments. *J. Agric. Food Chem.* **2007**, *55*, 5367–5376.
- (2) Diagne, M.; Oturan, N.; Oturan, M. A.; Sirés, I. UV-C light-enhanced photo-Fenton oxidation of methyl parathion. *Environ. Chem. Lett.* **2008**, doi: 10.1007/s10311-008-0162-1.
- (3) Stalikas, C. D.; Konidari, C. N. Analytical methods to determine phosphonic and amino acid group-containing pesticides. *J. Chromatogr. A* **2001**, *907*, 1–19.
- (4) Rueppel, M. L.; Brightwell, B. B.; Schaeffer, J.; Marvel, J. T. Metabolism and degradation of glyphosate in soil and water. *J. Agric. Food Chem.* **1977**, *25*, 517–528.
- (5) Borggaard, O. K.; Gimsing, A. L. Fate of glyphosate in soil and the possibility of leaching to ground and surface waters: A review. *Pest Manage. Sci.* **2008**, *64*, 441–456.
- (6) Barrett, K. A.; McBride, M. B. Oxidative degradation of glyphosate and aminomethylphosphonate by manganese oxide. *Environ. Sci. Technol.* **2005**, *39*, 9223–9228.
- (7) Baylis, A. D. Why glyphosate is a global herbicide: strengths, weaknesses and prospects. *Pest Manage. Sci.* **2000**, *56*, 299–308.
- (8) Duke, S. O.; Powles, S. B. Glyphosate: A once-in-a-century herbicide. *Pest Manage. Sci.* **2008**, *64*, 319–325.
- (9) Duke, S. D. In *Herbicides—Chemistry, Degradation and Mode of Action*; Kearney, P. C., Kaufman, D. D., Eds.; Marcel Dekker: New York, 1988.
- (10) Cox, C. Glyphosate: Herbicide factsheet. *J. Pest. Reform* **2004**, *24*, 10–15.
- (11) Kolpin, D. W.; Thurman, E. M.; Lee, E. A.; Meyer, M. T.; Furlong, E. T.; Glassmeyer, S. T. Urban contributions of glyphosate and its degrade AMPA to streams in the United States. *Sci. Total Environ.* **2006**, *354*, 191–197.
- (12) Huston, P. L.; Pignatello, J. J. Degradation of selected pesticide active ingredients and commercial formulations in water by photo-assisted Fenton reaction. *Water Res.* **1999**, *5*, 1238–1246.
- (13) Chen, Y.; Wu, F.; Lin, Y.; Deng, N.; Bazhin, N.; Glebov, E. Photodegradation of glyphosate in the ferrioxalate system. *J. Hazard. Mater.* **2007**, *148*, 360–365.
- (14) Shifu, C.; Yunzhang, L. Study of the photocatalytic degradation of glyphosate by TiO_2 photocatalyst. *Chemosphere* **2007**, *67*, 1010–1017.
- (15) Nowack, B.; Stone, A. T. Manganese-catalyzed degradation of phosphonic acids. *Environ. Chem. Lett.* **2003**, *1*, 24–31.
- (16) Aquino Neto, S.; de Andrade, A. R. Electrooxidation of glyphosate herbicide at different DSA compositions: pH, concentration and supporting electrolyte effect. *Electrochim. Acta* **2008**, *54*, 2039–2045.

- (17) Rajeshwar, K.; Ibanez, J. G. *Environmental Electrochemistry: Fundamentals and Application in Pollution Abatement*; Academic Press: San Diego, CA, 1997.
- (18) Oturan, M. A. An ecologically effective water treatment technique using electrochemically generated hydroxyl radicals for in situ destruction of organic pollutants: Application to herbicide 2,4-D. *J. Appl. Electrochem.* **2000**, *30*, 475–482.
- (19) Rodrigo, M. A.; Michaud, P. A.; Duo, I.; Panizza, M.; Cerisola, G.; Cominellis, C. Oxidation of 4-chlorophenol at boron-doped diamond electrode for wastewater treatment. *J. Electrochem. Soc.* **2001**, *148*, D60–D64.
- (20) Qiang, Z.; Chang, J.-H.; Huang, C.-P. Electrochemical regeneration of Fe^{2+} in Fenton oxidation process. *Water Res.* **2003**, *37*, 1308–1319.
- (21) Wang, A.; Qu, J.; Ru, J.; Liu, H.; Ge, J. Mineralization of an azo dye Acid Red 14 by electro-Fenton's reagent using an activated carbon fiber cathode. *Dyes Pigm.* **2005**, *65*, 227–233.
- (22) Da Pozzo, A.; Merli, C.; Sirés, I.; Garrido, J. A.; Rodríguez, R. M.; Brillas, E. Removal of the herbicide amitrole from water by anodic oxidation and electro-Fenton. *Environ. Chem. Lett.* **2005**, *3*, 7–11.
- (23) Friedman, C. L.; Lemley, A. T.; Hay, A. Degradation of chloroacetanilide herbicides by anodic Fenton treatment. *J. Agric. Food Chem.* **2006**, *54*, 2640–2651.
- (24) Yuan, S.; Tian, M.; Cui, Y.; Lin, L.; Lu, X. Treatment of nitrophenols by cathode reduction and electro-Fenton methods. *J. Hazard. Mater. B* **2006**, *137*, 573–580.
- (25) Sirés, I.; Garrido, J. A.; Rodríguez, R. M.; Brillas, E.; Oturan, N.; Oturan, M. A. Catalytic behavior of the $\text{Fe}^{3+}/\text{Fe}^{2+}$ system in the electro-Fenton degradation of the antimicrobial chlorophene. *Appl. Catal., B* **2007**, *72*, 382–394.
- (26) Flox, C.; Garrido, J. A.; Rodríguez, R. M.; Cabot, P. L.; Centellas, F.; Arias, C.; Brillas, E. Mineralization of herbicide mecoprop by photoelectro-Fenton with UVA and solar light. *Catal. Today* **2007**, *129*, 29–36.
- (27) Sáez, C.; Panizza, M.; Rodrigo, M. A.; Cerisola, G. Electrochemical incineration of dyes using a boron-doped diamond anode. *J. Chem. Technol. Biotechnol.* **2007**, *82*, 575–581.
- (28) Sirés, I.; Brillas, E.; Cerisola, G.; Panizza, M. Comparative depollution of mecoprop aqueous solutions by electrochemical incineration using BDD and PbO_2 as high oxidation power anodes. *J. Electroanal. Chem.* **2008**, *613*, 151–159.
- (29) Sirés, I.; Guivarch, E.; Oturan, N.; Oturan, M. A. Efficient removal of triphenylmethane dyes from aqueous medium by in situ electro-generated Fenton's reagent at carbon-felt cathode. *Chemosphere* **2008**, *72*, 592–600.
- (30) Oturan, M. A.; Guivarch, E.; Oturan, N.; Sirés, I. Oxidation pathways of malachite green by Fe^{3+} -catalyzed electro-Fenton process. *Appl. Catal., B* **2008**, *82*, 244–254.
- (31) Pimentel, M.; Oturan, N.; Dezotti, M.; Oturan, M. A. Phenol degradation by advanced electrochemical oxidation process electro-Fenton using a carbon felt cathode. *Appl. Catal., B* **2008**, *83*, 140–149.
- (32) Nowack, B. Environmental chemistry of phosphonates. *Water Res.* **2003**, *37*, 2533–2546.
- (33) Motekaitis, R. J.; Martel, A. E. Metal chelate formation by *N*-phosphonomethylglycine and related ligands. *J. Coord. Chem.* **1985**, *14*, 139–149.
- (34) Subramaniam, V.; Hoggard, P. E. Metal complexes of glyphosate. *J. Agric. Food Chem.* **1988**, *36*, 1326–1329.
- (35) Watts, R. J.; Sarasa, J.; Loge, F. J.; Teel, A. L. Oxidative and reductive pathways in manganese-catalyzed Fenton's reactions. *J. Environ. Eng.* **2005**, *131*, 158–164.
- (36) Le Fur, E.; Colin, R.; Charrêteur, C.; Dufau, C.; Péron, J.-J. Determination of glyphosate herbicide and aminomethylphosphonic acid in natural waters by liquid chromatography using pre-column fluorogenic labeling. Part I: Direct determination at the 0.1 $\mu\text{g/L}$ level using FMOC. *Analisis* **2000**, *28*, 813–818.
- (37) Zhu, Y.; Zhang, F.; Tong, C.; Liu, W. Determination of glyphosate by ion chromatography. *J. Chromatogr. A* **1999**, *850*, 297–301.
- (38) Anipsitakis, G. P.; Dionysiou, D. D. Radical generation by the interaction of transition metals with common oxidants. *Environ. Sci. Technol.* **2004**, *38*, 3705–3712.
- (39) Hanna, K.; Chiron, S.; Oturan, M. A. Coupling enhanced water solubilization with cyclodextrin to indirect electrochemical treatment for pentachlorophenol contaminated soil remediation. *Water Res.* **2005**, *39*, 2763–2773.
- (40) Haag, W. R.; Yao, C. C. D. Rate constants for reaction of hydroxyl radicals with several drinking water contaminants. *Environ. Sci. Technol.* **1992**, *26*, 1005–1013.

Received for review January 26, 2009. Accepted April 27, 2009.